Milena BEDLA-PAWLUSEK[a], Robert PASTUSZKO[b, *], Robert KANIOWSKI[b]

[a] Holy Cross Cancer Center, Kielce, Poland
[b] Faculty of Mechatronics and Mechanical Engineering, Kielce University of Technology, Poland
* Corresponding author: tmprp@tu.kielce.pl

COMPARISON OF POOL BOILING HEAT TRANSFER COEFFICIENTS FOR SURFACES WITH OPEN MICROCHANNELS OF VARIABLE AND CONSTANT DEPTHS

Key words: pool boiling, microchannels, visualization.

Abstract: Experimental studies of pool boiling heat transfer on open microchannels of variable and constant depth were conducted. Microchannels of variable depth from 0.05 to 2.8 mm and a width from 0.2 and 0.5 mm were uniformly spaced on base surfaces with a pitch of 0.4 and 1.0 mm. Reference surfaces with microchannels with a constant depth were 0.2 or 0.4 mm wide and 0.2 or 0.5 mm deep. The experiment was conducted for three liquids, i.e. water, ethanol, and Novec-649, at atmospheric pressure. A comparison of heat transfer coefficients (HTCs) for surfaces with microchannels of constant and variable depths was made. The highest values of the heat transfer coefficient for boiling water were obtained for microchannels with a constant depth at heat flux above 350 kW/m^2. At the boiling of ethanol, the highest HTCs were achieved at a heat flux above 150 kW/m^2 for narrow microchannels with variable depths. A high speed camera and photo camera were used to record images of the entire sample surface. Visualization investigations were aimed at identifying nucleation sites and determining the bubble growth cycle.

Porównanie współczynników przejmowania ciepła dla powierzchni z otwartymi mikrokanałami o zmiennej i stałej głębokości

Słowa kluczowe: wrzenie w dużej objętości, mikrokanały, wizualizacja.

Streszczenie: Przeprowadzono eksperymentalne badania wymiany ciepła przy wrzeniu w mikrokanałach o zmiennej i stałej głębokości. Mikrokanały o zmiennej głębokości od 0,05 do 2,8 mm i szerokości 0,2 i 0,5 mm były równomiernie rozmieszczone na powierzchni podstawy z podziałką 0,4 i 1 mm. Powierzchnie referencyjne wykonano w postaci mikrokanałów o stałej głębokości 0,2 lub 0,5 mm oraz szerokości 0,2 lub 0,4 mm. Eksperyment był prowadzony dla następujących czynników wrzących: wody, etanolu i Novec-649, będących pod ciśnieniem atmosferycznym. Najwyższe wartości współczynnika przejmowania ciepła podczas wrzenia wody uzyskano dla mikrokanałów o stałej głębokości przy gęstości strumienia ciepła powyżej 350 kW/m^2, natomiast przy wrzeniu etanolu najwyższe wartości współczynnika przejmowania osiągnięto przy zastosowaniu wąskich mikrokanałów o zmiennej głębokości, dla gęstości strumienia ciepła powyżej 150 kW/m^2. Do zarejestrowania obrazów na całej powierzchni próbki użyto kamery o wysokiej prędkości i aparatu cyfrowego. Badania wizualizacyjne miały na celu zarejestrowanie obrazów miejsc tworzenia, wzrostu i oderwania się pęcherzyków.

Introduction

This article concerns experimental research on boiling heat transfer on new structured surfaces with microchannels. The aim of this article is to compare heat transfer coefficients for surfaces with microchannels of variable and constant depths.

The analysed surfaces can be used for cooling elements or systems that generate high heat fluxes, including electronics, as well as in evaporators (as a thermosiphon or tubular evaporator), air conditioning devices, and heat exchangers.

The dissipation of large amounts of heat is required when working with many technically advanced

devices, including heat exchangers for hydrogen storage, advanced radar, X-ray medical equipment, supercomputers, computer data centres, hybrid vehicle power electronics aircraft, satellite and spacecraft avionics, and laser and microwave directed energy weapons [1].

Electronic devices are the main part of mechatronics systems. The development of electronics is limited by efficient cooling, which is necessary to operate mechanisms in the desired temperature range. For heat fluxes above 1 kW/m², traditional air cooling methods based on free or forced convection become unsuitable for most applications. Air-cooled systems often do not meet the cooling needs of the complicated electronic devices due to the low values of heat transfer coefficients. Because of the latent heat during the phase change, pool and flow boiling have an advantage over one-phase systems [2].

Pool boiling is an effective cooling technique due to its ability to remove large heat fluxes at low superheats, i.e. temperature difference between wall temperature and saturation liquid temperature. Heat exchangers using pool boiling are applied in the following applications: power generation, chemical, pharmaceutical, petrochemical, and process industries [3], as well as in refrigeration and air conditioning, electric power plants, and high-integrated electronic chip devices [4]. Pool boiling heat transfer in a confined space has been used in the cooling systems of high-power semi-conductors in high speed trains (e.g., TGV) [5].

Numerous scientific publications deal with the nucleate pool boiling on extended surfaces (channels, tunnels, fins). Jaikumar and Kandlikar [6] conducted research on heat transfer on the surface in the form of microchannels with porous fin tops. The channels were 300–760 μm wide and 200–400 μm deep. The tests were carried out for the FC-87 working fluid at atmospheric pressure. For a microchannel with a width and depth of 400 μm, the highest heat transfer coefficient (HTC) 20 kW/(m²K) was achieved. Kwak et al [4] conducted experimental studies of pool boiling on high aspect-ratio microchannels. Heating surfaces with open rectangular microchannels with various channel heights (10, 20, 50, and 100 μm) and a channel width of 30 μm were investigated. The authors found that boiling HTC enhanced with an increment in microchannel depth. Heat transfer coefficients of up to 60 kW/(m²K) were obtained.

Investigations of pool boiling on surfaces with microchannels and microfins were carried out by Gouda, Pathak, and Khan [7]. The 10 x 10 mm² samples were made of copper. The tests were carried out under atmospheric pressure for deionized water. The authors observed that microfin structures showed better heat transfer performance compared to the surfaces with open microchannels. A heat transfer coefficient of about 120 kW/(m²K) was obtained for surfaces with microchannels.

Kaniowski and others [8] conducted experimental research on copper samples with microchannels with depths of 0.2–0.4 mm and widths of 0.3 mm for two working fluids: water and Novec-649. The largest HTC for water and for Novec-649 was 64 kW/(m²K) and 8 kW/(m²K), respectively.

This article focuses on the comparison of boiling efficiency of enhanced structures in the form of microchannels (0.05–2.8 mm in depth) with constant and variable depths. The purpose of the study was to find the optimal geometry of microchannels for the highest heat transfer coefficient during water and ethanol boiling.

1. Experimental setup

Figure 1 shows a diagram of the measuring stand for determining the boiling curves. The main stand module (Fig. 2) consists of a vessel with four flat glass walls, filled with boiling liquid and placed over the sample under test. The sample was soldered to a cylindrical cooper bar that was 45 mm in diameter and 170 mm in length. A 1200 W electric cartridge heater, 19 mm in diameter and 130 mm in length, was installed inside the cooper bar. Figure 3 shows thermocouple arrangement. Eight K type thermocouples (NiCr-NiAl) of 0.5 or 1.0 mm in diameter were placed as follows: in the liquid (T1, T2), under the sample (T3, T4), and in the bar at 5, 10, 20, and 35 mm depths (T5 – T8).
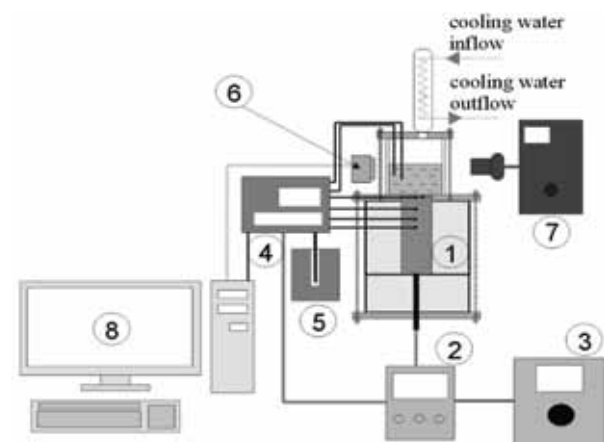

Fig. 1. Measurement system: 1 – main module, 2 – wattmeter, 3 – autotransformer, 4 – data logger, 5 – dry-well calibrator, 6 – high speed camera/digital camera, 7 – light, 8 – PC

Data reduction was achieved based on [9]. The heat flux was determined from the temperature gradient in the upper part of the heating cylinder, assuming one-dimensional heat conduction (Fig. 3)

$$q = \frac{\lambda_{Cu}\Delta T_{5\text{-}8}}{l_{5\text{-}8}} \qquad (1)$$

Due to the shift of the temperature measurement point, the extrapolated superheat was as follows:

$$\Delta T = T_{3\text{-}4,m} - \frac{q \cdot l_e}{\lambda_{Cu}} - T_{sat} \qquad (2)$$

where $T_{3\text{-}4,m}$ denotes the mean temperature measured by the two thermocouples in the sample base (T3 and T4) and l_e – is the distance between the microchannel bottom and thermocouples under the sample. The saturation temperature T_{sat} was determined as an average of temperature readings from two thermocouples (T1 and T2, Fig. 3) embedded in the boiling fluid.

The heat transfer coefficient was expressed as follows:

$$\alpha = \frac{q}{\Delta T} \qquad (3)$$

The estimated uncertainties were as follows:
- Low heat flux (3.5 kW/m²): heat flux ±35%, heat transfer coefficient ±40%.
- High heat flux (600 kW/m²): heat flux ±1.1%, heat transfer coefficient ±2%.
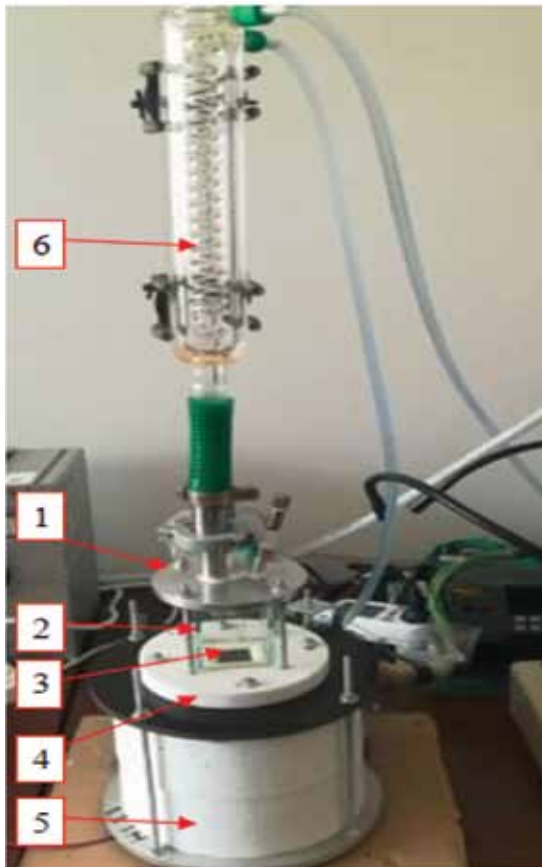
2. Experimental surfaces

Experimental studies were conducted for two types of samples:
- Open microchannels with variable depths: MCV-0.5-0.2_2.8-1.0 and MCV-0.2-0.05_1.7-0.4; and,
- Open microchannels with constant depths MC-0.4-0.5-0.8, MC-0.2-0.2-0.4 and MC-0.2-0.3-0.4.

The samples were made of copper on the basis of a square with a side of 27 mm, with an increased dimension of the base to 32 mm. Figure 4 shows one of the tested MCV surfaces, and Figure 5 presents one of the MC surfaces. Table 1 compiles geometrical parameters of surfaces with constant and variable depths. The designation code (w-h_{min}–h_{max}-p) is the following: the first number denotes the microchannel width in mm (w), the second number is the minimum microchannel depth (h_{min}), the third one denotes maximum microchannel depth (h_{max}), and the fourth number is the microchannel pitch (p).
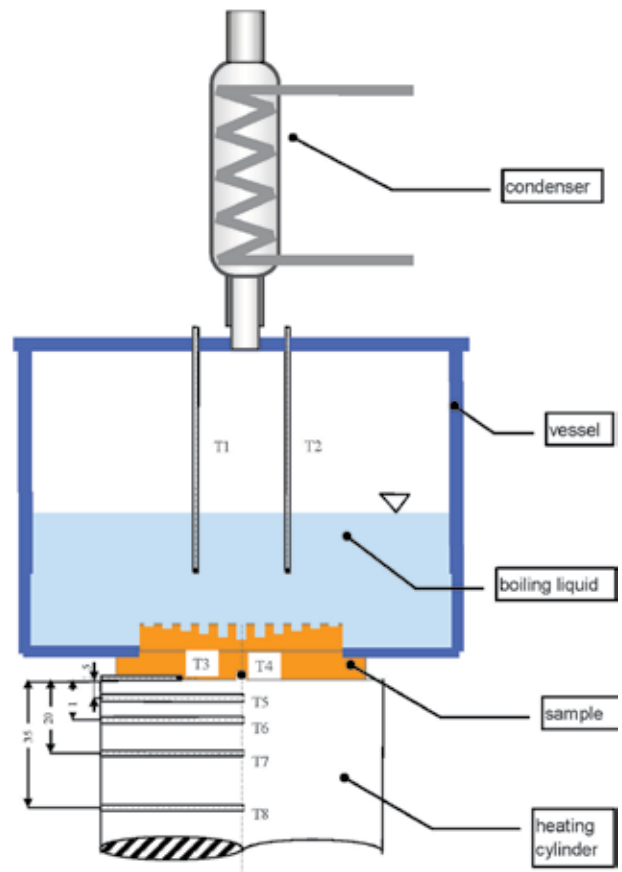

Fig. 2. **Main module: 1 – top flange, 2 – glass vessel, 3 – sample, 4 – Teflon annular flange, 5 – insulation, 6 – condenser**

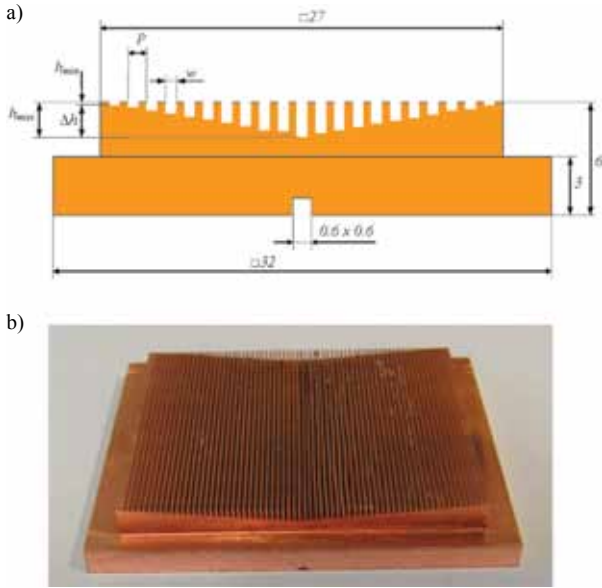Fig. 3. **Arrangement of thermocouples**

a)

b)

Fig. 4. Cross section (a) and photograph (b) of the sample MCV-0.2-0.05_1.7-0.4
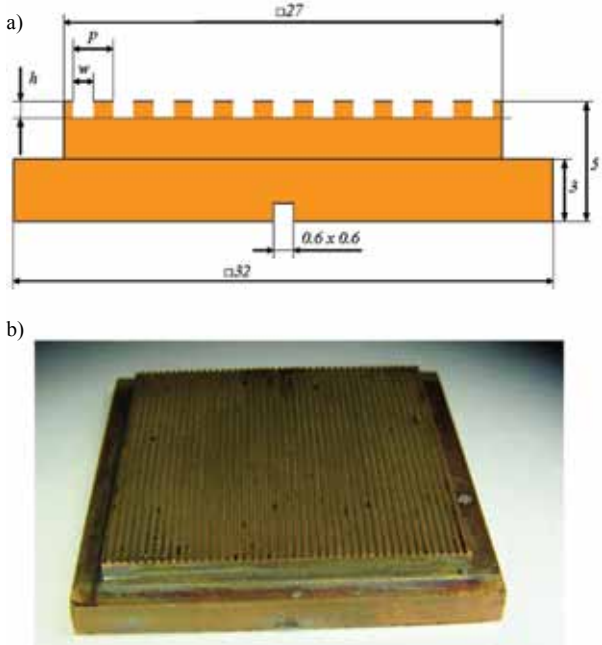
a)

b)

Fig. 5. Cross section (a) and photograph (b) of the sample MC-0.2-0.2-0.4

Table 1. Surfaces codes and specifications

Sample code	w mm	h_{min} mm	h_{max} mm	Δh mm	p mm
MCV-0.5-0.2_2.8-1.0	0.5	0.2	2.8	0.2	1.0
MCV-0.2-0.05_1.7-0.4	0.2	0.05	1.7	0.05	0.4
MC-0.4-0.5-0.8	0.4	0.5	0.5	0.0	0.8
MC-0.2-0.2-0.4	0.2	0.2	0.2	0.0	0.4
MC-0.2-0.3-0.4 (only visualization)	0.2	0.3	0.3	0.0	0.4

3. Heat transfer coefficients (HTCs)

Surfaces with open microchannels were tested for two different liquids – water and ethanol. Only additional visualization tests were carried out for the working fluid Novec-649.

Figures 6 and 7 illustrate the dependence of the heat transfer coefficient on the heat flux for boiling water and ethanol.

The largest HTC at the boiling of water, about 45 kW/(m²K), was obtained for microchannels with a constant depth of 0.2 mm (Fig. 6). For both tested samples with variable depths, with heat flux q = 19 – 180 kW/m², almost identical heat transfer coefficients were obtained. For MCV-0.5-0.2_2.8-1.0 samples at bigger heat fluxes, q > 200 kW/m², higher heat transfer coefficients were obtained compared to the sample MCV-0.2-0.05_1.7-0.4. In the heat flux range of 360 – 490 kW/m², almost constant values of HTC were obtained for a sample with a smaller depth change, i.e. MCV-0.2-0.05_1.7-0.4. Both samples, compared to a sample with a smooth surface, achieved better heat transfer coefficients.

However, in comparison to open microchannels with constant depth, for boiling water, both surfaces with variable depths achieved higher HTCs for q < 250 kW/m². For q > 400 kW/m², both microchannels with constant depth achieved better heat transfer coefficients compared to samples with variable depths.

When low heat fluxes were used, below q < 100 kW/m², for boiling ethanol, very similar values of the heat transfer coefficient were obtained for both the samples with variable and with constant depths (Fig. 7). In contrast to the boiling water, for heat flux above 150 kW/m², the highest HTCs were achieved for narrow microchannels with variable depths (MCV-0.2-0.05_1.7-0.4).
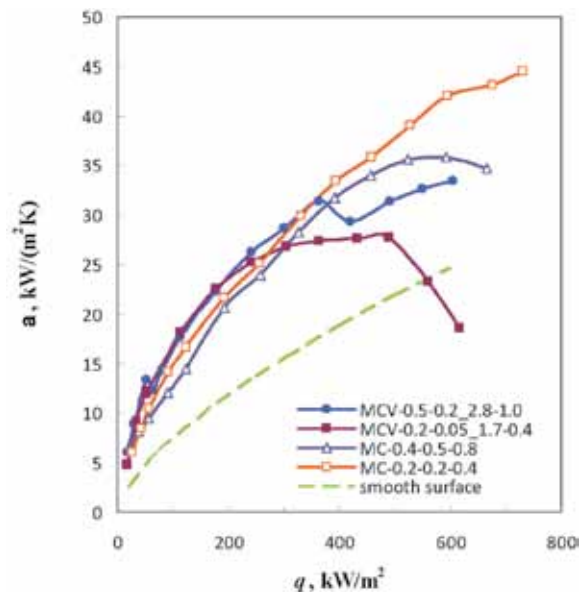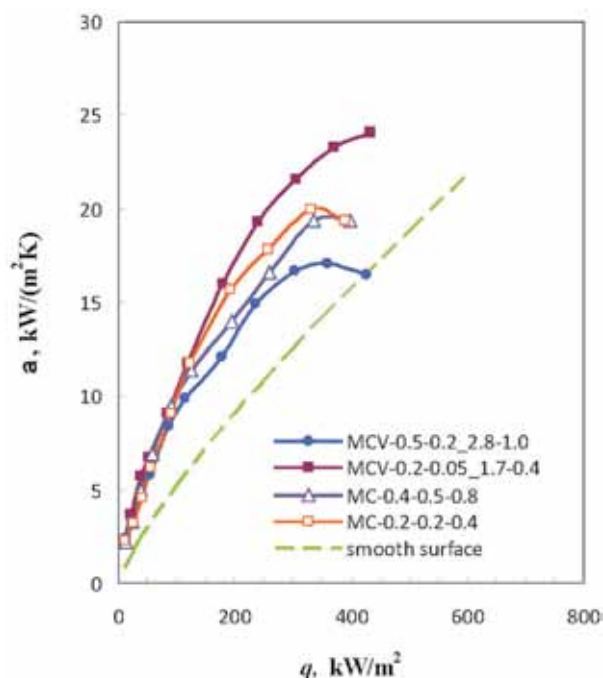

Fig. 6. Boiling curves for water

Fig. 7. Boiling curves for ethanol

4. Visualization of boiling

The mechanism of bubble formation, their growth, and detachment is shown in Figures 8–12. Figures 8 and 10 show the boiling fluid visualization for the MCV-0.5-0.2_2.8-1.0 sample, and Figures 9 and 11 for the MCV-0.2-0.05_1.7-0.4 sample. Figure 12 presents a bubble growing on the surface with constant depth microchannels (MC-0.2-0.3-0.4).

The bubble formation cycle takes place inside the microchannel. The nucleation sites, i.e. the places of the vapour bubble generation, constitute the corners between the bottom of the microchannel and the lateral surface of the microfin forming the microchannel limitation. Figures 8a, 8b, 10a, 11a, and 12a show a growing bubble adhering to the bottom of the microchannel. Figures 8c, 9a, and 12b show enlarged bubbles that fill the entire space of the microchannel. The surplus of the buoyancy force in relation to the surface tension force causes the bubbles to move towards the tops of the microfins (Figures 8d, 8e, 9b, 10b, 11b, and 12c). A further bubble growth can be observed on the microfins tips (Figures 9c, 9d, 10c, 10d, 11c, 11d, and 12d).

Figures 13–15 show active nucleation site areas for boiling ethanol on the surfaces with 0.2 mm wide variable depth microchannels. At low heat fluxes, there are higher wall temperatures at the bottom of the central microchannels, which results in the intense formation and detachment of bubbles in this zone (Fig. 13). Smaller overheating in external microchannels results in a low intensity of bubble generation (flooding mode, i.e. the advantage of liquid inflow than evaporation). It can be

observed that external channels are activated gradually at medium heat fluxes (Fig. 14), and, at higher heat fluxes (Fig. 15), all microchannels are active. In addition, intensive coalescence takes place above microfin tops.
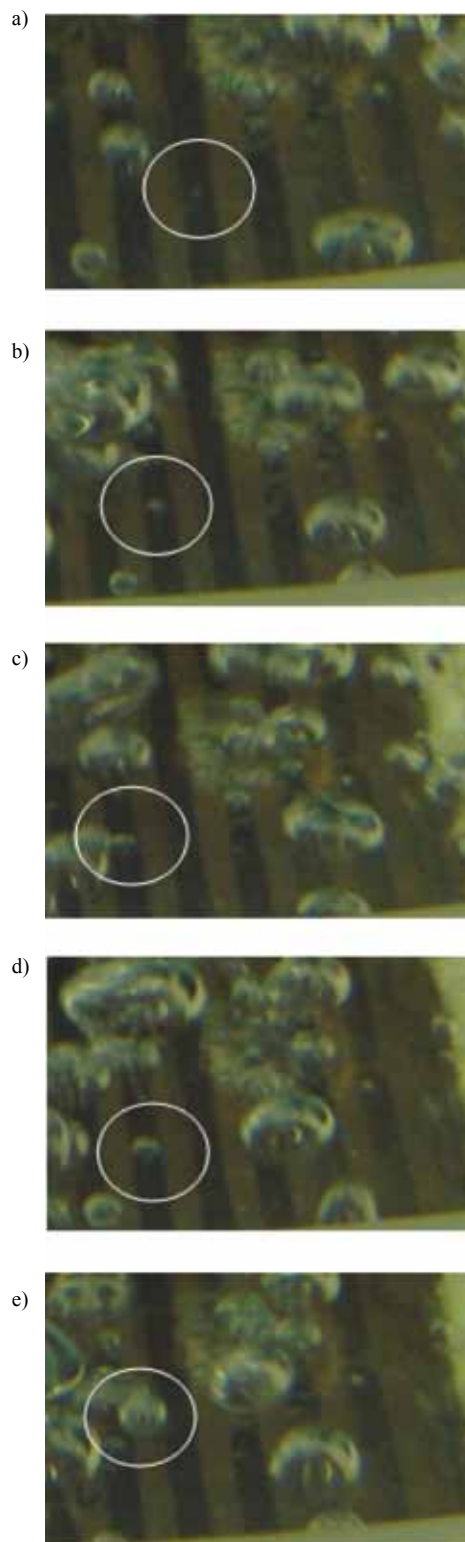

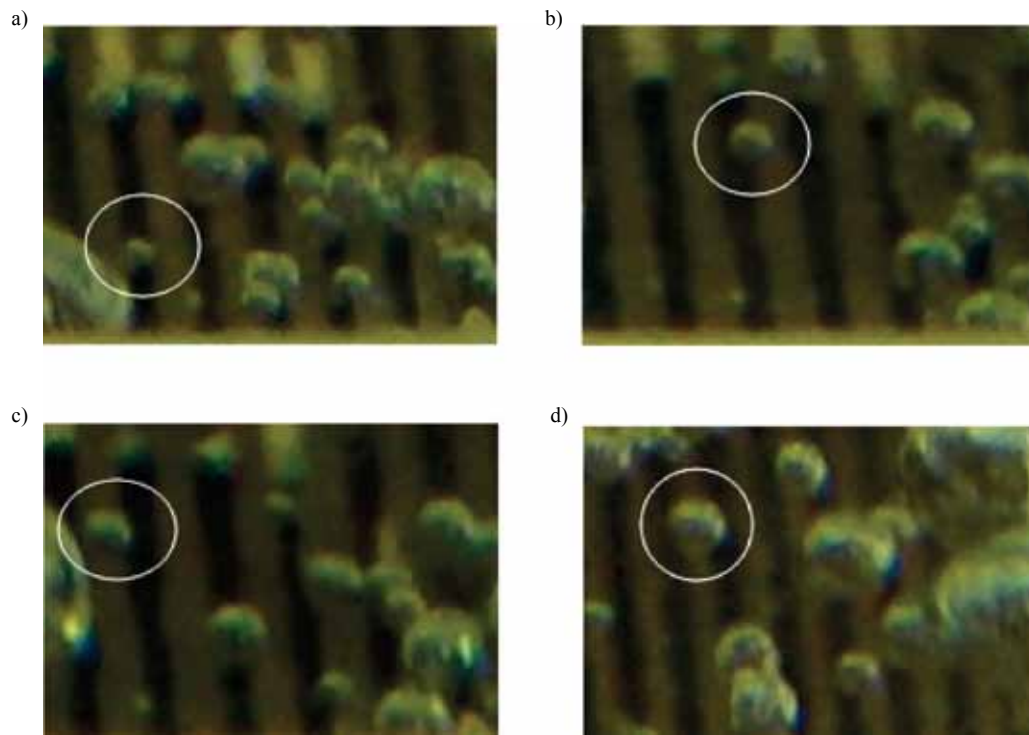**Fig. 8. Visualization of pool boiling of ethanol on the microchannel surface MCV-0.5-0.2_2.8-1.0, $q = 22.8$ kW/m²**

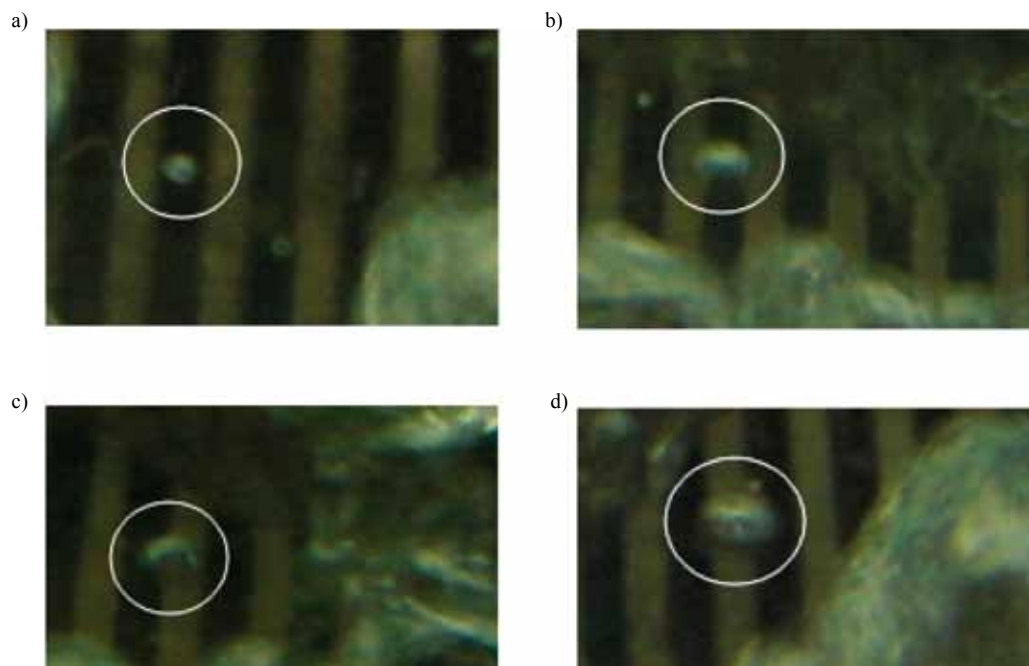Fig. 9. Visualization of pool boiling of ethanol on the microchannel surface MCV-0.2-0.05_1.7-0.4, $q = 21.5$ kW/m²

Fig. 10. Visualization of pool boiling of water on the microchannel surface MCV-0.5-0.2_2.8-1.0, $q = 30.4$ kW/m²
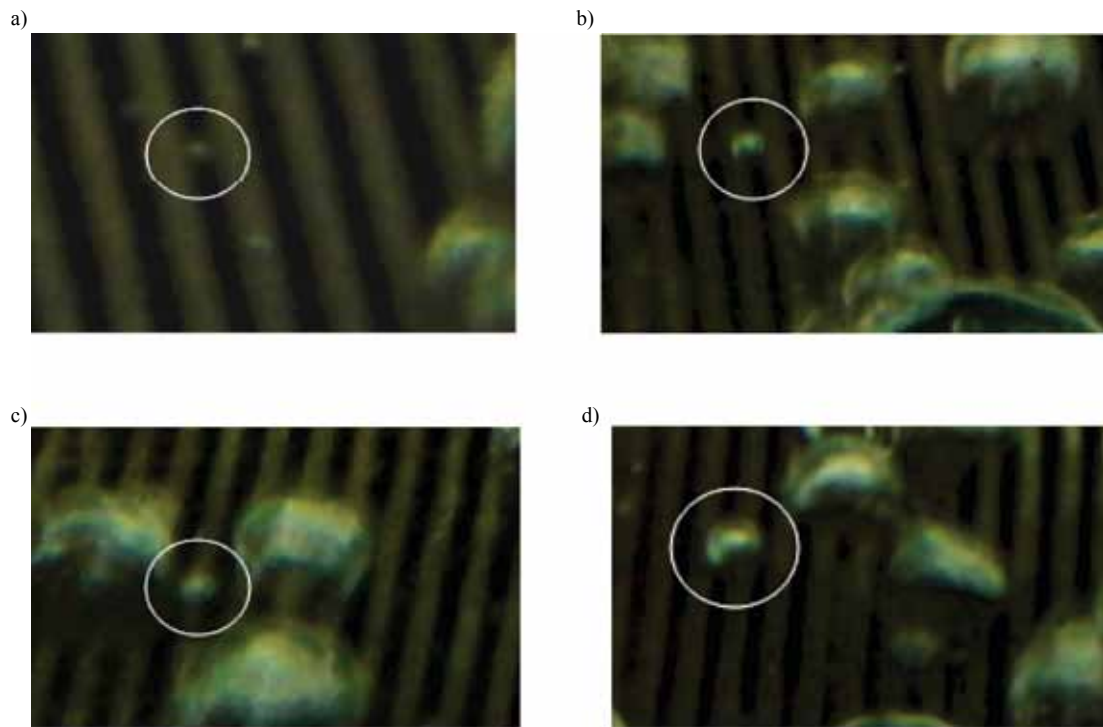
a)

b)

c)

d)

Fig. 12. Visualization of pool boiling of Novec–649 on the microchannel surface MC-0.2-0.3-0.4, $q \approx 3.5$ kW/m

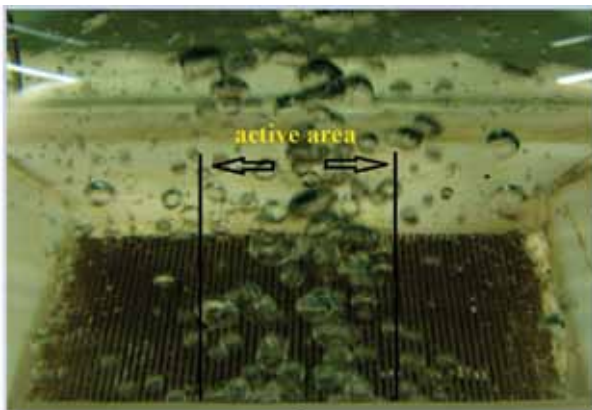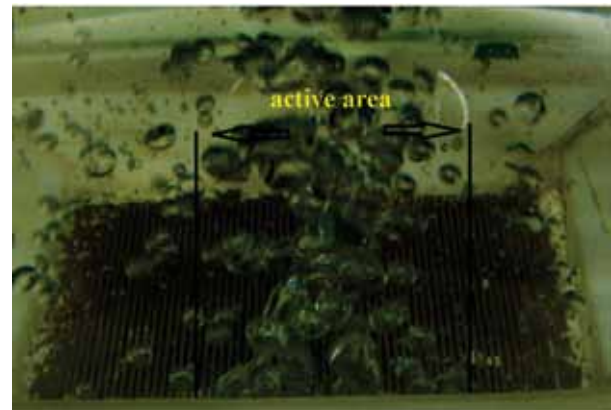**Fig. 13. Active area for boiling ethanol at $q = 10.1$ kW/m²**

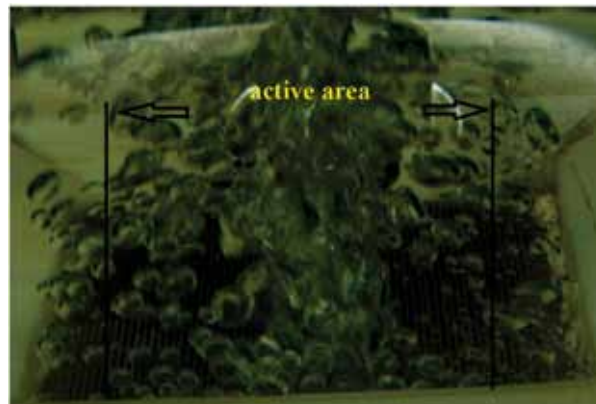**Fig. 14. Active area for boiling ethanol at $q = 21.5$ kW/m²**

Fig. 15. Active area for boiling ethanol at $q = 38$ kW/m²

Figure 16 shows the predicted boiling mechanism for microchannels of variable depths at low and high heat flux. Deep microchannels will contribute to the onset of nucleate boiling at low superheating; however, at higher heat flux heat transfer coefficient decreases after dry-out heat flux is reached. Microchannels with smaller depth improve the pool boiling performance at higher heat flux when the nucleating bubble activity is intense due to the availability of additional nucleation sites at higher superheating of the microchannels walls.
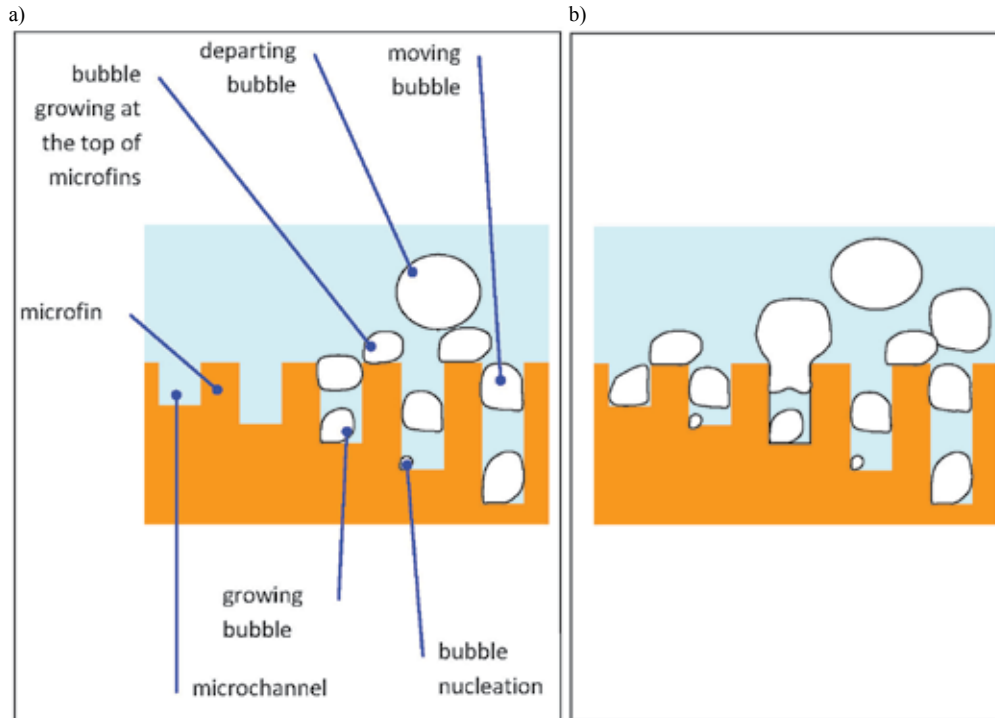

Fig. 16.   **Predicted pool boiling mechanism: bubbles nucleation, growing and departure in microchannels of variable depth; a) small heat fluxes, b) higher heat fluxes**

Conclusions

The following conclusions can be drawn from the experimental studies carried out:

- At small heat fluxes (below 300 kW/m² for water and below 100 kW/m² for ethanol), there are only slight differences between the heat transfer coefficients for the four tested surfaces.
- The highest values of the heat transfer coefficient for boiling water were obtained for a sample with constant microchannel depths of 0.2 mm (MC-0.2-0.2-0.4) at a heat flux above 350 kW/m².
- At boiling of ethanol, the highest heat transfer coefficients were achieved at a heat flux above 150 kW/m² for narrow microchannels with variable depths (MCV-0.2-0.05_1.7-0.4).
- Visualization of the research allowed the presentation of the initial assumptions of the model of bubble formation and growth for the analysed structure.
- More exact conclusions can be drawn after testing a larger number of samples with MC and MCV surfaces in the width range of 0.3–0.6 mm.
- The analysed surfaces can be used as thermosiphon or heat pipe evaporators.

Nomenclature

h – depth, m,
HTC – heat transfer coefficient,
l – distance, m,
MC – microchannel,
MCV – microchannel with variable depth,
p – pitch, m,
q – heat flux, kW/m²,
T – temperature, K,
w – width, m,

Greek symbols

α – heat transfer coefficient, W/(m²K),
λ – thermal conductivity, W/(mK),
Δh – change of depth, m,
ΔT – difference of temperature, K,

Subscripts

Cu – copper,
e – extrapolation,
m – mean,
min – minimum,
max – maximum,
sat – saturation.

References

1. Liang G., Mudawar I.: Review of pool boiling enhancement by surface modification. *International Journal of Heat and Mass Transfer*, 2019, 128, pp. 892–933.
2. Tullius J.F., Vajtai R., Bayazitoglu Y.: A review of cooling in microchannels. *Heat Transfer Engineering,* 2011, 32, pp. 527–541.
3. Patil C.M., Kandlikar S.G.: Pool boiling enhancement through microporous coatings selectively electrodeposited on fin tops of open microchannels. *International Journal of Heat and Mass Transfer,* 2014, 79, pp. 816–828.
4. Kwak H. J., Kim J. H., Myung B., Kim M. H., Kim D. E.: Behavior of pool boiling heat transfer and critical heat flux on high aspect-ratio microchannels. *International Journal of Thermal Sciences,* 2018, 125, pp. 111–120.
5. Bonjour J., Lallemand M.: Effects of confinement and pressure on critical heat flux during natural convective boiling in vertical channels. *International Communications in Heat and Mass Transfer*, 1997, 24, pp. 191–200.
6. Jaikumar A., Kandlikar S.: Enhanced pool boiling for electronics cooling using porous fin tops on open microchannels with FC-87. *Applied Thermal Engineering.,* 2015, 91, pp. 426–433.
7. Gouda R.K., Pathak M., Khan M.K.: Pool boiling heat transfer enhancement with segmented finned microchanels structured surface. *International Journal of Heat and Mass Transfer,* 2018, 127, pp. 39–50.
8. Kaniowski R., Pastuszko R., Nowakowski Ł.: Effect of geometrical parameters of open microchannel surfaces on pool boiling heat transfer. *EPJ Web Conf.*, 2017, 143, 02049.
9. Pastuszko R., Wójcik T.M.: Experimental investigations and a simplified model for pool boiling on micro-fins with sintered perforated foil. *Experimental Thermal and Fluid Science*, 2015, 63, pp. 34–44.